Energy Conversion and Management 258 (2022) 115530

Contents lists available at ScienceDirect

Energy Conversion and Management

journal homepage: www.elsevier.com/locate/enconman

Novel methodology for performance characterization of vertical axis wind turbines (VAWT) prototypes through active driving mode

Luis Santamaría *, Jesús Manuel Fernández Oro, Katia María Argüelles Díaz, Andrés Meana-Fernández, Bruno Pereiras, Sandra Velarde-Suárez

Fluid Mechanics Area, Department of Energy, University of Oviedo, C/Wifredo Ricart s/n, Gijon, Asturias 33204, Spain

ARTICLE INFO

Keywords:
Vertical axis wind turbine
VAWT
Wind tunnel
Performance characterization
Active driving mode

ABSTRACT

Vertical axis wind turbines (VAWT) are called to have an important role in the definitive penetration of renewable energies in the near future. Although still under development, they are considered good candidates for urban environments and offshore generation in deep waters. For its experimental characterization, wind tunnel testing of small-scaled VAWTs is usually employed. However, self-starting issues, reduced aerodynamic torques -for reliable measurement- and high rotational speeds -imposed by similarity- emerge as inherent operative problems. To overcome these issues, Active Driving Mode (ADM) is commonly used to drive the turbine under equivalent kinematic conditions introducing an external motor. Up to now, an accurate characterization of the turbine performance, in terms of retrievable aerodynamic power, is not available for this methodology in the open literature.

This work presents the development and application of an innovative methodology for testing VAWT prototypes through ADM. Interesting advantages over the conventional determination of the turbine performance using Passive Driving Mode (PDM) are shown. It is demonstrated that a deep level of characterization and high-test control is achieved with a simple experimental set-up. In addition, the key aspects for the application of this methodology have been identified and studied in detail, like the isolation of the mechanical losses from the blade drag or the quantification of the parasitic drag of the turbine struts. Relevant conclusions have been revealed concerning the marginal effect of the induction factor on the parasitic drag, or the importance of a correct blade drag estimation for the computation of the mechanical losses. Finally, the methodology has been applied to a real wind tunnel set-up, for the characterization of a 3-bladed VAWT with a H-rotor based on the DU 06-W-200 profile. The performance results obtained experimentally have been accurately compared to CFD simulations.

1. Introduction

Nowadays, global energy models are increasingly focused on renewable energy sources and decentralized energy generation. Over the last two decades, wind energy has proven to be economical and reliable, being Horizontal Axis Wind Turbines (HAWT) one of the pillars of new energy policies due to its mature development. According to the International Energy Agency (IEA), by 2050, wind power will account for 19% (stated policies scenario STEPS) to 39% (net zero scenario NZE) of total world energy supply [1]. However, as the energy mix is more participated by renewable technologies, like solar PV or wind power, its variable power supply requires the development of new methods to adjust the production to the real-time demand curves. This issue is promoting the rise of a new energy economy based on microgrids and energy storage systems like batteries, small hydro reservoirs [2], CAES systems [3] or hydrogen, capable to provide distributed and variable energy integration. With those solutions, the energy supply is decoupled from the renewable sources, so local intermittencies, shortages due to weather conditions or occasional failures are also minimized. The adaptation of other types of variable renewable technologies, still under development and currently penalized by their difficult integration to the existing grid, can be even favored. Furthermore, in the current context, self-consumption for individual and collective installations is a growing approach in residential buildings, which has been proved profitable even without subsidies [4].

Lift-based Vertical Axis Wind Turbines (VAWT) have attracted renewed attention in recent times because they are particularly well-suited for this new scenario. Although they were already developed in

* Corresponding author.
E-mail address: santamarialuis@uniovi.es (L. Santamaría).

https://doi.org/10.1016/j.enconman.2022.115530
Received 13 January 2022; Received in revised form 23 February 2022; Accepted 21 March 2022
Available online 31 March 2022

the 70 s and 80 s, they were progressively abandoned due to the higher efficiencies and rated power provided by the HAWT family. Nevertheless, VAWTs characteristics make them better candidates than HAWTs for application in urban environments, due to their omnidirectionality, avoiding the need for orientation mechanisms; their ability to work better in variable wind conditions; and their lower noise emission [5]. In the case of wind turbines for offshore generation in deep waters, VAWTs are also a considerable option and specifically tailored to floating devices, due to their superior energy density for wind farming. In addition, VAWTs present a lower inclining moment, lower turbine mass and lower center of gravity which leads to more economical supporting structures [6]. Furthermore, they present their gearbox and generator at ground level which makes the operation easier and safer [7]. This is very important for offshore applications where deployment and maintenance labors in a sea environment are extremely difficult.

However, despite the valuable potential of VAWTs, their current state of development is still limited [8], mainly due to their complex aerodynamics. For its further study, wind tunnel testing is an essential tool to obtain reliable data. It allows direct visualization of flow-turbine interactions and provides experimental data for validation of both analytical and computational fluid dynamics (CFD) models. From an engineering point of view, wind tunnel data is also used to retrieve performance curves which are further extrapolated to real scale turbines.

Typically, the scale of the turbines has to be significantly downsized in order to preserve high tunnel-to-prototype size ratios. This leads to substantial reductions in the physical variables to be measured (i.e., power and torque), and high rotational speeds to match dynamic similarity. The mechanical losses and inertial effects are no longer marginal, so the prototype operation is compromised and the measurement of the aerodynamic power complicated. Moreover, conventional methodologies for performance characterization use passive elements such as brakes or generators to modify the operating point of the wind-driven turbines. The torque is measured directly with torquemeters [9] or other passive elements like Prony [10] or electromagnetic brakes [11] which over-increase the mechanical resistance. Additional torque control systems are also required to measure positive torque gradients in the torque-speed ratio curve, thus restricting the testable operating range even more [12]. As a result, the experimental wind tunnel tests of small-scale turbines in a passive driving mode (PDM) suffer from severe inconveniences and are not fully operational, being even aggravated with the self-starting issues of these kinematic turbines.

As a feasible alternative, active driving mode (ADM) tests, also called motor-driven, may be employed to avoid all these self-starting problems and small-scale issues. This option emerges when the turbine is not able to generate net power at the required rotating velocity, so the operating point is artificially achieved with an external energy input. The aerodynamic performance can be retrieved from that deficit, assuming that both situations are similar. Although this approach initially raised some concerns about its validity, Araya and Dabiri concluded that turbine wakes in the relevant operating range are independent from the driving mode [13]. They compared wake measurements of turbines in both motor-driven (ADM) and flow-driven (PDM) tests taken from several references and conducted their own study using PIV in a water channel. The limit of the application of this procedure was stablished at high TSRs where aerodynamic equilibrium between drag and lift is achieved. Recently, Dou et al. have also determined that unsteady flows and turbulence measured with hot-wire anemometry in a HAWT are identical using PDM or ADM [14]. So far, in the field of VAWT study, ADM has been employed mainly to run experiments at small scale for flow studies. Some examples can be found in the literature for the analysis of turbine flow using PIV techniques [15–17]. However, in those situations, the overall performance of the turbines is not provided, or, in best cases, it is obtained from additional tests with different experimental set-ups.

Both PDM and ADM provide an indirect measurement of the aerodynamic variables. In the case of PDM, the use of segregating routines to isolate the aerodynamic torque is already a common practice in the literature. However, up to the authors' knowledge, no formal method has been presented yet for ADM. Hence, the establishment of an accurate methodology to obtain the performance curves of lab-scale turbines under ADM would be really useful, allowing to finally circumvent all those previous limitations. It will also provide a more comprehensive way of analyzing flow visualization studies, relating them adequately with complementary performance measurements.

This paper presents the development of a novel methodology to characterize VAWT performance in active driving mode for wind tunnel testing at small scales. Although some references can be found regarding the employment of ADM for turbine characterization, a rigorous description on the application of this methodology is not available yet. A detailed process that may quantify the relevance of the different contributions is thus required. Some previous studies [18] briefly mention driving the turbine without flow to obtain a "tare" torque, but without subtracting parasitic drags. Other authors [13] are even disregarding the mechanical losses in the retrieval of the performance curves. This may lead to an excessive overestimation of the net aerodynamic power. Only using a well-posed method to decouple the different factors allows a correct estimation of the real values. This is the basic contribution of this research. In addition, it contributes to improve the practical study of low-solidity, high-efficiency turbines, which are essential for the above-mentioned applications. The methodology highlights for its moderate infrastructure, low instrumentation costs, easy-implementation, and reasonable degree of accuracy. This is particularly interesting for industrial-commercial application, where large-scale wind tunnels or high-cost instrumentation may not be accessible. This tool also allows a fast and simple utility to complement CFD studies and contribute to the ongoing growth of the VAWTs sector.

The methodology has been developed using an electric DC motor as the active element for the turbine control. The aerodynamic performance was obtained indirectly by the comparison of the supplied torque for different test conditions. Precisely, a remarkable effort has been made to isolate the aerodynamic torque from the mechanical losses and the parasitic drag of the struts. Note that this makes the methodology proposed here of special interest for the validation of analytical models or CFD simulations, in which the effect of the turbine structure or the blades struts is not usually considered. At the same time, a relevant part of the work was devoted to identifying the most problematic stages of the methodology, with special emphasis on those aspects requiring an in-depth study.

This work is structured as follows. First, the experimental set-up used is presented in Section 2, including the description of the measurement procedures. Then, Section 3 describes the development of the novel methodology, going from its theoretical basis to a practical approach. Critical aspects requiring special attention are also identified. The methodology is applied to the current set-up, and final results are shown. Section 4 is devoted to further exploring a key aspect of the methodology: the isolation of the aerodynamic drag from the mechanical losses. Afterwards, the influence on the methodology of the drag coming from the turbine struts is evaluated in Section 5. Greater detail is provided to improve the initial considerations given in Section 3. In Section 6 the results obtained are compared to numerical results from CFD simulations and a correction for blockage, based on previous works found in the literature, is proposed. Finally, relevant conclusions and future works are provided in Section 7.

2. Experimental SET-UP

A small-scale prototype of a 3-bladed VAWT, with a H-rotor based on the DU 06-W-200 profile, has been recently designed [19], developed [20] and constructed [21] by the authors. These actions are within the context of a National Research & Development Plan to promote the use and implementation of renewable energies for an ecological transition and a sustainable development.

Preliminary flow measurements have been conducted in a medium-size, 30 kW closed-loop wind tunnel, with a large blockage ratio in the test section. They were mainly devoted to quantifying tunnel-turbine interaction effects for the development of specific blockage corrections. Though maximum blockage ratios of a 5–10% are desirable, it is a common practice to employ higher values. This fact is due to the extremely wide test sections required by that limitation in case of typical VAWT prototypes [22]. Consequently, it is necessary to correct the blockage effect in order to extrapolate the measured output power for real-scale turbines operating under free-field conditions. Precisely, as a crucial part of this procedure, the existing facility and retrieved data have been used in the development of an ADM methodology to characterize the performance of the scaled prototype for different tip speed ratios.

The present experimental database corresponds to a high-blockage set-up, used to apply the proposed methodology for the performance characterization of VAWTs. Hence, the results must be considered only in the specific context of the research and may not be representative of the turbine design for expected characteristics in an actual wind environment. The reader is reminded to stay focused on the description and applicability of the methodology, of general use for wind tunnel testing. Hence the available data must be considered as a simple framework to exemplify its use.

The experimental set-up available for the present investigation includes:

Wind Tunnel. The experiments were conducted in the "XAWT" (*Xixón Aeroacustic Wind Tunnel*) located in the facilities of the Fluid Mechanics Area of the University of Oviedo. It is a closed-loop wind tunnel, driven by a 30 kW axial fan in an impulsion layout, with a total length of 24.6 m and 8.3 m high (arranged in a vertical position, see Fig. 1**, left**). It has an aerodynamic test section of 1.05 × 1.25 m^2, immersed in an anechoic chamber of 4.2 m long and cross-sectional area of 4.45 × 2.80 m^2. A 9.5:1 contraction nozzle with a logarithmic derivative profile accelerates the flow towards the test section. This wind tunnel can achieve velocities up to 22 m/s, for a maximum Reynolds number of $1.7{\cdot}10^6$ (based on the nozzle hydraulic diameter), with a mean turbulence intensity around 0.7% [23].

For the current research under high-blockage conditions, a hybrid modular enclosure has been used to fulfil a semi-confined environment with no wake blockage (shown disassembled in Fig. 1**, right**). More details can be found in [21].

Prototype. The turbine tested is a small-scale model of a 3-bladed "H"-type VAWT, specifically developed for urban environments (Kumar et al., 2018). "H"-VAWTs (Darrieus with straight blades) present lower manufacturing costs than other VAWT architectures and achieve good efficiencies. Nowadays, they are a trending choice for this kind of applications. The prototype has a diameter of 0.8 m and features 3 blades with the DU 06-W-200 airfoil. The blade chord is 0.067 m, and the blade length is 0.6 m, resulting in an aspect ratio H/D = 0.75 and a solidity σ = 0.5. The main geometrical characteristics are summarized in Table 1. This model has been built combining standard commercial elements, like aluminium profiles and joints, with custom-made parts manufactured by Fused Deposition Modelling (FDM). Special care was taken in the layer direction to avoid fatigue failure and abrupt fracture because of bending and centrifugal loads. The blades feature an epoxy coating to improve surface roughness and increase blade strength. To reduce the drag on the struts, a low-drag aerodynamic profile (EPPLER 863 Strut Airfoil) was introduced to cover the interior cylindrical rods. Fig. 2 shows the turbine inside the test chamber of the wind tunnel.

For this measurement campaign, the prototype was operated in motor-driven arrangement using a 1 kW, permanent magnet DC, electric motor. It has been powered by a 30 V/10 A laboratory power supply, which has a built-in measuring system. Previously, the motor was experimentally characterized in an independent test bench to determine its torque constant, k_t. This will allow to obtain the motor torque directly from the electric current in the different turbine tests, avoiding the need for an additional torquemeter and thus decreasing transmission mechanical losses.

Instrumentation. The flow velocity for the tests was controlled in the wind tunnel nozzle (inlet–outlet) using a Kimo CP210-R differential pressure transducer with an operative range of ± 1000 Pa and temperature compensation. The measurement of temperature allowed the correction of the air density inside the wind tunnel, as a function of the atmospheric pressure checked on an analogic barometer. The turbine rotational speed was measured instantaneously using a digital tachometer connected to a data acquisition card. In addition, the intensity of the power supply was also measured and registered in the computer by means of a specific software for its operation and recording. Ad-hoc acquisition software was also employed for the signal of the tachometer. Finally, a post-processing program was developed in MATLAB to obtain the test results. A simplified diagram of the instrumented experimental set-up is shown in Fig. 3. The measuring uncertainties of the different sensors are listed in Table 2.

Experimental routines. The objective is to measure the electric current supplied to the motor, for different rotating velocities of the turbine, when the wind tunnel is operated at a constant flow velocity.

Table 1
Main characteristics of the prototype.

Airfoil profile	DU 06-W-200
Blade number (N)	3
Chord (c) [m]	0.067
Diameter (D) [m]	0.8
Blade length (H) [m]	0.6
Solidity $\left(\sigma = \frac{N{\cdot}c}{D/2}\right)$	0.5
Aspect ratio (H/D)	0.75

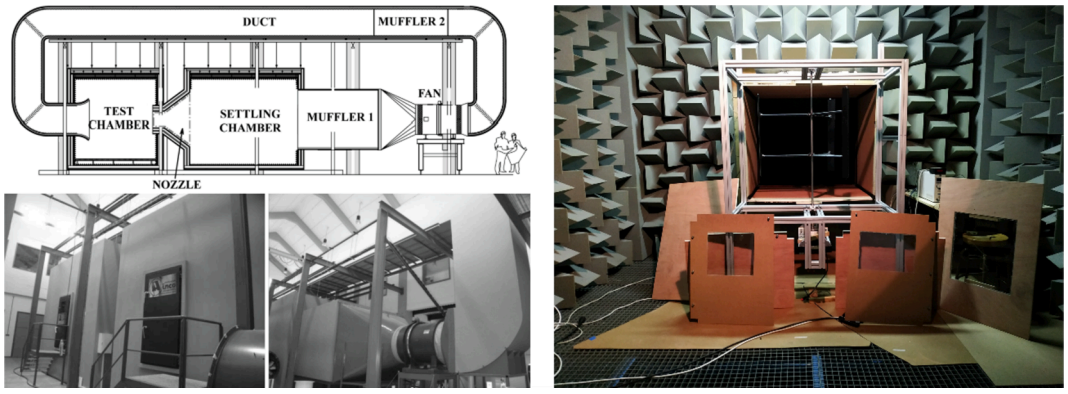

Fig. 1. XAWT wind tunnel (left). Aerodynamic test section with the turbine (right).

Fig. 2. Three-bladed H-VAWT installed inside an hybrid modular enclosure for the test chamber of the XAWT wind tunnel.

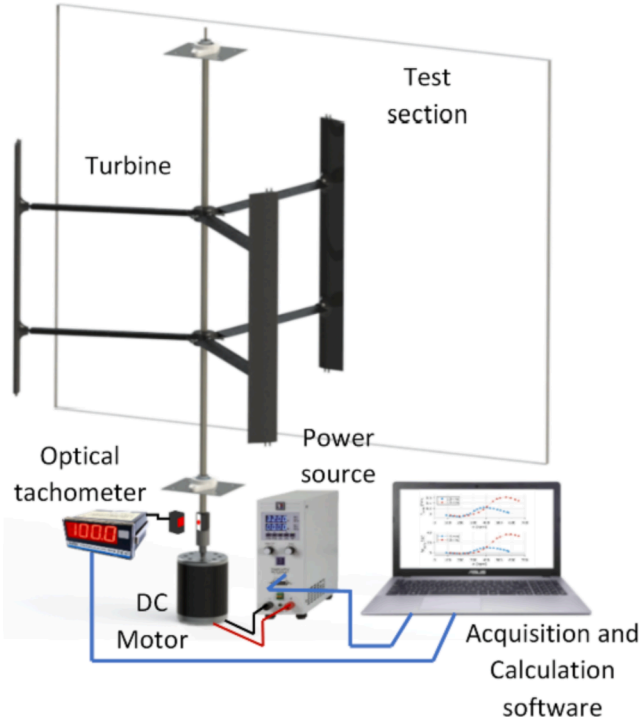

Fig. 3. Sketch with the experimental set-up and instrumentation used.

Table 2
Instrumentation uncertainties.

Sensor	Variable measured	Uncertainty
Differential pressure sensor Kimo CP210-R	Pressure difference	$u_{\Delta P} = \pm 0.005 \Delta P \pm 2[Pa]$
Optical tachometer	Rotational speed	$u_{\omega} = \pm 0.011 \left[\frac{rad}{s}\right]$
Laboratory power source Elektro Automatik PS 8360–10 T	Electric current	$u_I = \pm 0.01[A]$

The flow velocity in the wind tunnel is fixed regulating the flow rate delivered by the axial flow fan (opening/closing a set of louvers at the fan discharge). To modify the rotational speed of the motor-turbine assembly, the excitation of the DC motor is controlled by voltage regulation through the power supply, until the turbine reaches the desired rotational speed. The electric motor demands higher or lower current depending on the load, which varies with the rotational speed. Finally, the measurement is performed and stored after the prototype reaches a dynamic equilibrium.

The mechanical torque applied by the motor, T_{app}, is a function of the torque constant of the electric motor, k_t, the measured electric current, I, and a detrimental friction torque in the motor, T_f, according to:

$$T_{app} = k_t \cdot I - T_f \tag{1}$$

The friction torque depends on the speed of rotation and can be relevant at the wind tunnel scale, so it cannot be neglected. Nevertheless, the proposed methodology employs a sequence of different tests whose combined balance, in terms of torque, cancels out its influence for the final results. The complete procedure is detailed in the next section.

Note that for an accurate steady balance of the torques, the acquiring time of the measurements has to be maintained for a sufficiently extended period of time, so representative mean-time values can be obtained. Additionally, it is remarkable that the methodology described later is not dependent of the measuring instruments employed for the present work. In particular, the applied torque for equation (1) can be obtained directly from a torquemeter, thus suppressing the need for the experimental determination of the constant k_t. Alternatively, the electric current could have been measured using a high precision amperemeter/oscilloscope, instead of using the own utility of the power supply unit.

3. VAWT performance characterization in active driving mode (ADM)

The aerodynamic torque of a VAWT can be obtained indirectly from a motor-driven situation. To do so, similar fluid kinematic conditions to the wind-driven case must be satisfied and a precise subtraction of the system losses has to be performed. Precisely, a good estimation of the losses is the key point for the ADM to be really helpful for performance characterization. In the case of small-scale VAWTs in wind tunnels, this task can be quite challenging.

Two main sources of system losses can be identified in a conventional wind tunnel testing of a VAWT rotor. Firstly, mechanical losses arise due to bearing friction, transmission efficiencies in the couplings and even structural vibrations associated to slight misalignments and mass imbalances. Secondly, there are aerodynamic losses in the form of parasitic drag in the rotor struts. Additional aerodynamic losses can be accounted from blade-tip effects, although most authors consider them as a detrimental part of the aerodynamic efficiency of the rotor blades. Hence, they have been considered as a secondary flow of the blades for the present investigation, assuming that they are simply penalizing the rotor aerodynamics, instead of introducing further parasitic aerodynamic losses.

For the characterization of mechanical losses, two different approaches are suggested by the authors. The first approach is based on a turbine test that employs a rotor without blades, replicating similar conditions than a previous complete test with the blades mounted on the turbine. Under this condition, no aerodynamic power is generated. However, as the original bearing friction and mechanical resistance of the turbine is affected by the mass distribution of the rotor blades, the blade mass suppressed must be compensated with additional weights to maintain an equivalent structural behavior. This is difficult to implement in a realistic way without adding elements which produce new artificial aerodynamic losses. The second approach is based on a test where the turbine is driven without wind, thus avoiding additional disassembling operations. In this case, the main problem lays on how to isolate the mechanical losses from the aerodynamic drag torque due to the rotation of the blades. If that rotational drag is not discounted, it would result in an overestimation of the mechanical losses and of the aerodynamic torque. This second approach has been chosen by the authors for the present work, although the alternative option is also a

reliable possibility.

Regarding the second source for system losses, i.e. the parasitic losses drag in the struts, some recent works have employed analytical expressions to correct CFD results [24] for a better numerical estimation of VAWTs performance. For this work, an inverse insight is attempted through the isolation of the strut drag losses, leading to the retrieval of the aerodynamic power alone. This estimation can be later compared to CFD simulations. Note that due to the significant interaction of the blade wakes with the strut drag, an experimental approach may take into account this effect more easily. Therefore, two additional tests should be performed over the bladeless rotor comparing no wind conditions with respect to the inflow velocity situation. Its difference provides the estimation of the strut parasitic drag. However, this estimation is not considering the effect of the induction factor of the turbine when bladed, which may require an extra correction of the inflow velocity for the struts. Thus, the importance of this minor issue should be quantified.

Consequently, an effective procedure to evaluate the performance of a small-scale turbine under ADM on a wind tunnel experiment would require 2 main tests and 2 additional ones to account for strut parasitic drag. Note that the parasitic drag is rather relevant, especially in the case of typical prototype sizes. Hence, four tests were finally completed under different configuration and components, including:

Test 1. Whole turbine without wind.

Test 2. Whole turbine under constant wind velocity.

Test 3. Bladeless turbine without wind.

Test 4. Bladeless turbine under constant wind velocity.

As a result, Fig. 4 represents the evolution of the applied torque in the motor as a function of the rotational speed for all the tests performed. An inlet flow velocity of 7.5 m/s in the test section of the wind tunnel has been employed for tests 2 and 4. The solid lines account for tests with the complete turbine (1 and 2), while dashed lines correspond to the tests without turbine blades (3 and 4). Similarly, blue curves indicate tests with wind and black curves tests without wind. Tests 1, 3 and 4 (no aerodynamic power available) are fitted using a second-order polynomial (square markers) with a remarkable accuracy (RMSE less than 0.036, $R^2 > 0.9997$), as expected from the typical dependence of losses with rotational speed.

The different trend observed in the curve for test 2 evidences the effect of aerodynamic torque in the turbine performance. Firstly, with the turbine under stalled conditions, the set-up demands higher motor torque than in the no-wind situation. This corresponds to the velocity range between 100 and 250 rpm. Then, as the rotational speed is increased, the operating point of the turbine shifts to the positive torque

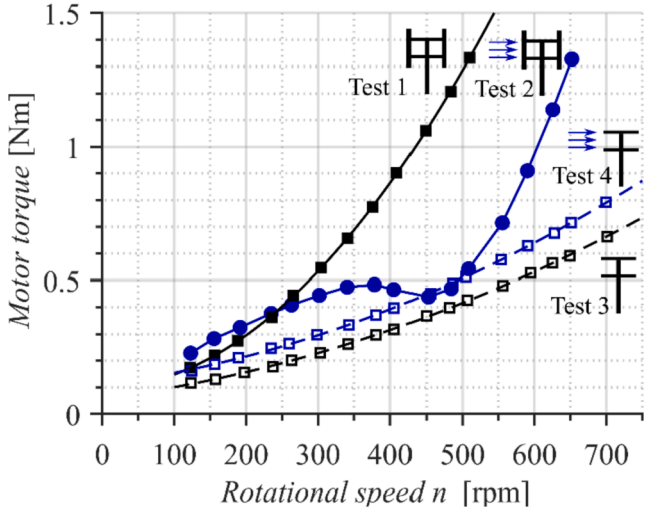

Fig. 4. Applied motor torque as a funtion of the rotational speed of the turbine for the different tests performed. Tests under wind conditions (2 and 4) were performed at 7.5 m/s inlet velocity.

generation zone, decreasing the demanded motor torque. In particular, the range between 350 (the local maximum) and 550 rpm (sudden increase of the slope) comprises that region. Finally, at high rotational velocities (higher than 550 rpm), the motor torque demand is significantly increased with a much stepper slope. At that final stage, the turbine is moving away from its optimal operating point and progressively declining its energy generation.

With that polynomial fits it is possible to evaluate the torques in the tests 1, 3 and 4 at the speeds corresponding to test 2. Following, the aerodynamic torque can be deduced with simple momentum equations in the shaft for the different cases. Firstly, the torque equilibrium for the complete turbine with no wind (test 1) yields:

$$T_{app_1} = T_{Db} + T_{Ds1} + T_{loss1} \tag{2}$$

where T_{app_1} is the applied torque by the electric motor, T_{Db} and T_{Ds1} are drag torques from the blades and struts respectively, and T_{loss1} is the friction torque associated to mechanical losses. Obviously, sub index 1 denotes the corresponding test. Similarly, for the second test the momentum equation leads to:

$$T_{app_2} + T_{aero} = T_{Ds2} + T_{loss1} \tag{3}$$

where T_{aero} represents the net aerodynamic torque provided by the blades. Note that, in this case, the mechanical losses, T_{loss1}, are identical to those found in the first test (both tests present the same machine configuration). On the contrary, the drag in the struts is not preserved because of its dependency to the incident relative velocity, which is function of the wind velocity and the rotational speed. Now, rearranging equation (2) to isolate the mechanical losses and substituting in equation (3), it is expressed as:

$$T_{aero} = \left(T_{app_1} - T_{app_2}\right) + \left(T_{Ds2} - T_{Ds1}\right) - T_{Db} \tag{4}$$

The term $(T_{Ds2} - T_{Ds1})$ in equation (4) can be easily obtained from the results given by tests 3 and 4. Since these tests correspond to the set-up with the bladeless turbine, the mechanical losses are different with respect to test 1 and 2, but equal between them. On the other hand, assuming that the struts drag is not modified between analogous tests of aerodynamic resistance (1–3 and 2–4), it can be easily expressed that:

$$T_{app_3} = T_{Ds1} + T_{loss3} \tag{5}$$

$$T_{app_4} = T_{Ds2} + T_{loss3} \tag{6}$$

After subtracting equations (5) and (6), it gives:

$$T_{Ds2} - T_{Ds1} = T_{app_4} - T_{app_3} \tag{7}$$

And finally, combining (4) and (7), it leads to this compact equation that includes all the torque data measured in the four tests:

$$T_{aero} = \left(T_{app_1} - T_{app_2} + T_{app_4} - T_{app_3}\right) - T_{Db} \tag{8}$$

In this expression, all the terms required to deduce the aerodynamic torque are known and represented in Fig. 4, expect for the last term, T_{Db}, which corresponds to the drag on the blades when the complete turbine is rotating under no wind conditions. Several possibilities can be employed to estimate this term. In particular, a 2D CFD simulation of a single rotating airfoil has been chosen as the best compromise between reliability and computational costs for the present application. More details and discussion are provided later in the next section.

The complete set of tests have been carried out for two different wind velocities, 5.5 and 7.5 m/s, in order to evaluate the reliability and functionality of this method. Higher velocities have not been employed to avoid possible mechanical failures in the prototype: an increment of the wind speed implies that the rotational speed must be increased linearly to fulfill dynamic similarity. This results in excessively high centrifugal forces compromising the structural integrity of the scaled turbine (for the lab materials and manufacturing methods employed).

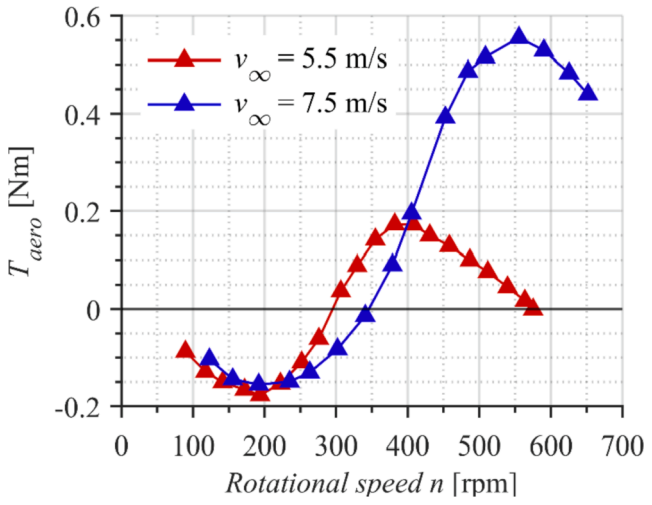

Fig. 5. Aerodynamic torque as a function of the rotational speed for two different wind velocities.

Fig. 5 shows the final results obtained of aerodynamic torque, as a function of the rotational speed of the turbine, for the two wind velocities tested.

Fig. 5 demonstrates that the developed methodology allows a thorough characterization of the performance, even at rotational velocities where the blades are stalled so the turbine does not produce positive torque. It is clearly revealed that the aerodynamic torque at these scales is not sufficient to exceed both mechanical losses and passive resistances. Hence, its measurement would be extremely difficult using conventional methods. Furthermore, it is manifested that the prototype is not able to surpass the cut-in threshold using only the wind force unless a motor-clutch driving system is provided. With the active driving mode these difficulties are overcome, and an accurate performance evaluation is obtained with a simple and cost-effective set-up. Moreover, the good control provided by the electric motor over the rotational speed of the turbine also allows to obtain a higher number of points than with conventional methodologies, even reducing the time required for the experimental tests.

To conclude this section, it is necessary to address the uncertainty of the instrumentation and its impact on the measuring procedures. Table 2 declares an uncertainty of $u_I = \pm 0.01[A]$ for the measurement of the electric current supplied by the power source. In addition, the torque constant has been determined with a relative uncertainty of $\frac{u_{k_t}}{k_t} = \pm 0.4[\%]$. The combined uncertainty of the resulting aerodynamic torque due to this instrumentation has been calculated following the procedure described in [25], which estimates a value of uncertainty transmitted through the measuring chain towards the desired variable. For the torque, it can be calculated according to:

$$u_{T_{aero}}(k_t, I) = \sqrt{\left(\frac{\partial T_{aero}}{\partial k_t}\right)^2 \cdot u_{kt}^2 + 4 \cdot \left(\frac{\partial T_{aero}}{\partial I}\right)^2 \cdot u_I^2} \tag{9}$$

For the test of 7.5 m/s reference velocity, it provides an uncertainty of ± 0.005 Nm for the maximum torque value, which in relative terms represents only a ± 0.9%. Note that it is a remarkable result, since the magnitude of the measured values is significantly small. Consequently, the accuracy verified, in combination with the affordable cost of these elements employed, dictates that the proposal is a rather interesting choice for the instrumentation of ADM tests.

Finally, further research efforts have been made over two key aspects of the methodology: a correct determination of the blades drag torque (the term T_{Db}); and a deep analysis of the influence of the wind velocity on the parasitic drag of the struts (on the term $T_{app_4} - T_{app_3}$). These topics are discussed in detail in Sections 4 and 5 respectively.

4. Isolating drag losses from mechanical ones

Under no wind situation, the drag on the airfoils is generated due to the circumferential velocity of the rotating blades. In the relative frame, it means that the inflow velocity can be assumed to be equal to the blade velocity with its direction tangential to the blade chord. Since the prototype tested corresponds to a rotor designed with zero-pitched blades, a 0 deg Angle-of-Attack (AoA) has to be considered. Note that this assumption is most accurate for low-solidity turbines, where the tangential distance between consecutive blades is large. In the case of high-solidities, the inflow velocity of every blade can be significantly affected by the wake deficit of the preceding blade, thus compromising the condition of uniform inlet flow.

In addition, if the radius of the turbine is at least one order of magnitude higher than the blade chord, it is also reasonable to consider that the aerodynamics of the blade are similar to that found in a linear cascade. Due to the absence of wind flow, the relative AoA is maintained during the whole turbine rotation, so drag coefficients can be taken directly from typical airfoil databases (like NREL reports, UIUC databases, etc.) or other published data for cascades. They can be also provided by low-order numerical programs like Xfoil, Javafoil or Rfoil among others. In the case that the required Re numbers are not available in the references, those programs allow easy extrapolation that can be attempted to obtain the values at the corresponding Re of the experiments.

However, in the case of small-scaled prototypes, the R/c ratio is usually reduced, compromising very seriously the assumption of equivalent flow to a linear cascade. Since the blades drag losses are very relevant for the correct computation of the aerodynamic torque, this is not a minor issue. In particular, for the present turbine with R/c = 6, it has been observed that the influence of rotational forces cannot be neglected, showing a severe impact on the evolution of the blade wakes and thus conditioning the final value of the drag loss. This has been observed through the simulation of the turbine airfoil, both in a linear cascade (LC) and a rotating cascade (RC). A 2D steady RANS simulation with a k-W SST turbulence modelling, recommended in the literature [26], has been employed for the purpose. Special attention has been paid to the spatial discretization of wall-adjacent mesh, with up to 450 nodes in the streamwise direction of the airfoil and further refinement in the normal direction to guarantee y+= 1 [27]. Since the flow at zero AoA is not suffering from detached conditions, unsteady computations or SRS turbulence modelling can be obviated. Conversely, additional options for curvature corrections and fully-swirl terms have been accounted in the resolution of the governing equations of the model with ANSYS Fluent v.17.2.

At this point, it is noted that it could be tempting to carry out the full 2D simulation of the whole turbine for its performance characterization. However, this implies extremely high computational costs, thus moving away from the initial objective of a low-cost, easy to implement methodology. A full simulation, even with a 2D model, of a typical VAWT requires high demanding unsteady simulations, with long-run executions and small time step sizes. This is mandatory to obtain a final fully-periodic simulation [26], as well as a high-order turbulence model to take into account all the vortical structures. Consequently, as a good compromise between economy and precision, a 2D simulation of a single rotating airfoil is finally proposed.

In Fig. 6, the vorticity normalized with the apparent wind velocity to chord ratio is shown in the vicinity of the airfoil for the two simulations. A typical Re number (based on the blade chord) equal to 100,000 has been selected for the analysis. In the upper map, the significant curvature of the blade wakes reveals the impact of the rotating effects. A comparison with the linear cascade map also shows how the turbulent wake is more pronounced in the internal side of the blades. These differences imply significant increments in the drag coefficients under rotation. This reveals that an accurate treatment of the drag losses is crucial for the estimation of the turbine performance.

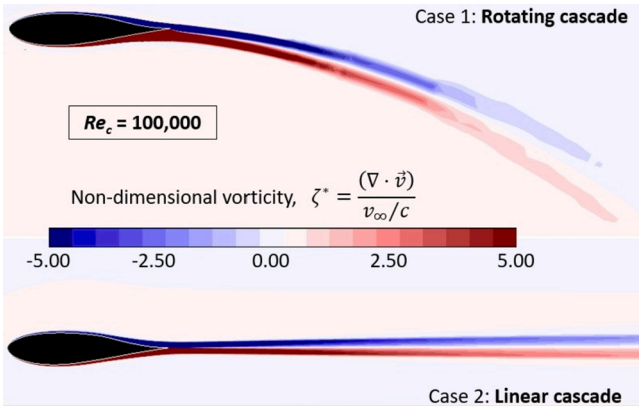

Fig. 6. Comparison of airfoil wakes obtained numerically with a rotating cascade (top) and a linear cascade (down).

Fig. 7 shows drag coefficients of the DU 06-W-200 airfoil for different Re numbers at 0 deg AoA, taken from various references in the literature (Rfoil, Xfoil and [28]). As expected, the available data is out-of-range for the small-scale experiments, so a power fit (black dashed line) was employed to extrapolate the coefficients at the required Reynolds numbers ($2.3{\cdot}10^4$ to $1.2{\cdot}10^5$, in the case of the 7.5 m/s test). In addition, drag coefficient values from both static 2D linear cascade (blue squares) and rotating cascade (red diamonds) simulations have been added to the representation. Note that at high Reynolds numbers ($Re > 3{\cdot}10^5$), the results from the bibliography are coincident with the values obtained from the LC simulation.

At Reynolds numbers lower than $5{\cdot}10^4$, the results from the different curves diverge significantly, although they are placed in a region with marginal impact in the estimation of the blades drag loss for the methodology (due to the low value of the rotational velocities). On the contrary, in the range from $5{\cdot}10^4$ to $1.2{\cdot}10^5$, the observed differences in Fig. 7 are lower, but their final relevance is more important. For example, at a tip-speed ratio of 2.6 (equivalent to $Re = 9{\cdot}10^4$) the power coefficient calculated from CFD-RC estimations differs around an 8% from those provided with the CFD-LC approach, and even a 12% using the extrapolated values from the references. Furthermore, at a tip-speed ratio of 3.5 (equivalent to $Re = 1.2{\cdot}10^5$), the differences increase up to 16% and 32% respectively.

Despite the significant disparities in the estimation of the drag coefficients, no alternative method with sufficient reliability has been found in the literature. On the contrary, the mechanical losses are frequently not considered or even grossly estimated. Therefore, depending on the desired level of accuracy, it is the user responsibility to decide the most convenient approximation to its particular set-up.

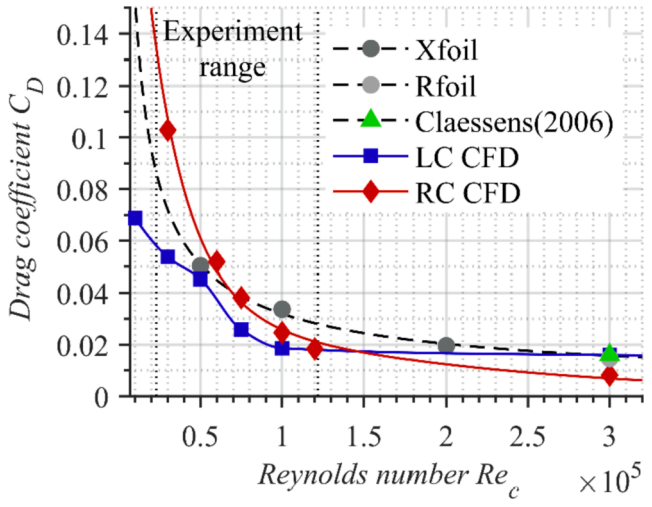

Fig. 7. Comparison of DU 06-W-200 drag coefficients for different approaches.

5. Parasitic strut drag

The parasitic drag of the turbine struts is the second key factor in the characterization of VAWTs performance in ADM. It is an important mechanism for resistant torque so it must be properly accounted to obtain reliable results.

In previous section 3, it was already discussed that strut parasitic drag can be easily isolated in ADM by performing the comparison between wind and no wind tests for the bladeless turbine (test 3 vs test 4). However, a concern was raised about the difference in the wind velocity perceived by the struts due to the induction factor when the turbine is bladed against when it is not. To analyze this question, the applied torque was measured for test 4 at three different wind velocities (v_∞ = 5.5, 7.5 and 10 m/s), and compared to the results for no wind velocity ($v_\infty = 0$) of test 3 (Fig. 8).

As a starting point, the figure demonstrates an evident quadratic dependence on the rotational velocity for the resistant torque of the struts in all the tests. Also, there is a linear evolution between the tests at 5.5, 7.5 and 10 m/s, showing the same vertical increment between the curves. It is noticeable, in the case of no wind velocity for test 3 (v_{inf} = 0), that the difference of this curve with respect to the others is progressively deviating from linearity as rotational velocity increases. However, this is a quite marginal effect, associated to the self-induced blockage of the turbine structure for high rotational speed on the cases with inflow velocity. More important is the difference in the struts drag between test 3 at zero velocity and any other curve of test 4, really significant at these small scales, even for the present prototype in which the struts are streamlined with low drag airfoils of thickness around 2% of the turbine span. Hence, this shows that accounting for parasitic strut drag is critical at wind tunnel scales, especially in case of prototypes with non-aerodynamic struts (although it is usually neglected, as reported in [22]).

Furthermore, there is an additional consideration for the estimation of this parasitic drag of the struts which needs further discussion. When the struts are rotating isolated from the blades (i.e., tests 4), the incoming velocity perceived by the struts is practically coincident to the inflow velocity from the wind tunnel section. However, when the full turbine is operated (test 2), the flow deceleration within the turbine (generated by the aerodynamics of blades and typically quantified as an induction factor) reduces the actual inlet velocity acting on the struts, thus modifying the net aerodynamic torque.

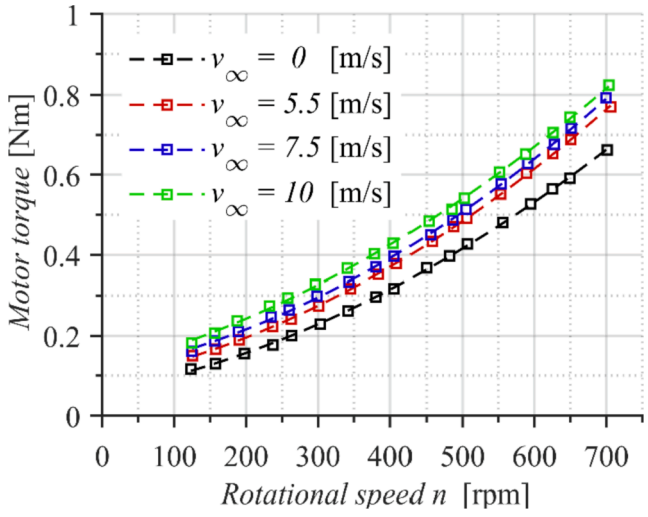

Fig. 8. Applied torque as a function of the rotating speed. Comparison between results for test 3 and test 4 at three different wind velocities.

In other words, to take into account the effect of the decelerated flow induced by the blades over the parasitic drag of the struts, it would be necessary to apply in equation (8) the torque of an equivalent test 4, T^{eq}_{app4}, operated with a reduced, "apparent" incoming velocity. Depending on the tip-speed ratio, this induction factor (relating the apparent and original inflow velocities) could represent a velocity reduction between 5 and 40% for a typical turbine design [19]. Unfortunately, this value cannot be easily known a priori, and it is also dependent on the particular characteristics of the turbine (geometry, struts design, solidity, airfoil family, etc.).

To estimate the importance of this effect, the final aerodynamic torque provided by this turbine (in the case of 7.5 m/s) is obtained introducing different parasitic torques – T^{eq}_{app4} in equation (8) –, retrieved from different apparent inflow velocities. The deviation from the result obtained without considering any correction is provided in Table 3 for nominal conditions (maximum available torque).

As expected, the higher the induction factor, the higher the difference in percentage. Significant discrepancies are observed for the highest flow deceleration, reaching up to 8.7% in the case of an induction factor equivalent to 0.4. However, the impact of this effect is sufficiently small (less than 3% at MTP and 5% at MVP) for low-to-moderate induction factors (below 0.2), indicating that it can be obviated maintaining a reasonable accuracy. Only in case of high-blocked turbines, with induction factors starting from 0.4, it is recommended to introduce this correction in the methodology to update the values of the resistant torque of the struts.

6. Comparison with CFD models

In this final section, the obtained performance results from the turbine are compared with complementary results from numerical simulations, as an example of real application and also for validation purposes. In particular, the results corresponding to a wind velocity of 7.5 m/s have been used for the comparison.

Firstly, a complete 2D URANS model of the VAWT turbine positioned on the extended casing of the wind tunnel nozzle (Fig. 9) has been developed with the objective of replicate the performance curve. A mesh density with the same requirements that the single-airfoil RC model was employed, resulting in a [450 × 40] O-mesh distribution over the blades and a total number of 350,000 cells for the whole domain. The sliding mesh technique was employed to resolve the rotational motion of the turbine, with a variable time-step size equivalent to 0.25 deg of angular displacement for every tip-speed ratio. At least, five complete rotations of the turbine were necessary to assure the periodic response of the aerodynamic torque. Similar k-ω SST turbulence modelling, discretization schemes and resolution algorithms to the RC simulation were employed.

In order to compare the results of this 2D CFD model with the real 3D experimental curves, it is necessary to introduce some scaling factors to take into account the vertical clearance of the turbine (H = 0.6 m) with respect to the casing height (L = 1.05 m). Calculating the ratio of the volumetric flow rates in both 2D and 3D situations (in 2D, the flow rate is per unit length; whereas in 3D it is considering the real transversal section), and assuming that it must be similar, a scaling factor for the tip-speed ratios between the 2D and 3D cases is obtained. On the other hand, considering the cubic dependence of the power coefficient with respect to the bulk velocities, a scaling factor for the power values can be also derived, yielding to:

$$\lambda_{3D} = \lambda_{2D}\frac{H}{L} \tag{10}$$

$$C_{p,3D} = C_{p,2D}\left(\frac{H}{L}\right)^3 \tag{11}$$

A complete range of equivalent tip-speed ratios, going from 1.5 to 3.9, have been simulated for an inlet velocity of 7.5 m/s in order to obtain the aerodynamic power curve of the turbine. As an illustration of the results, distributions of vorticity are represented in Fig. 10 for three different tip-speed ratios (2.1, 3.0 and 3.9) in a non-dimensional form (relative to the turbine rotating speed). Typical vortex shedding is identified in the development of the blade wakes, being more pronounced for lower tip-speed ratios. Thus, at 2.1, the turbine wake is more distorted, due to the downstream transport of the big vortices shed from the turbine blades, especially in the leeward region. Note also the relevant vortex shedding generated downstream of the turbine shaft. As the tip-speed ratio is increased, the boundary layers are more attached to the blades and the overall level of unsteadiness is reduced, including a weakened Von Kárman vortex street shed from the cylindrical shaft. The lateral casing prevents the widening of the turbine wake in all the cases. Moreover, an interaction between the vortices shed from the lateral shear layers of the turbine wake and the shear stress of the lateral walls is clearly established. As the turbine rotation is further increased (for TSR values of 3 and 3.9), a lateral high-jet region is progressively observed with a mitigation in the vortex shedding from the lateral casing but with a higher fluctuation for the overall wake.

With the factors defined in eq. (10) and (11), the performance results obtained from the 2D modelling (in terms of mean aerodynamic torque as a function of the TSR value) are transformed into the equivalent curve for a full 3D case. Hence, typical power coefficient, defined as $C_P = 2\dot{W}_{aero}/\rho v_\infty^3 HD$, are represented in Fig. 11 as a function of the tip-speed ratio, $\lambda = \omega D/2v_\infty$, for the present numerical simulations and compared to the experimental values of the set-up shown previously in Fig. 5. In particular, the corrected CFD results are shown as black squares in the figure, while experimental results are represented as blue triangles, with a remarkable level of agreement between them. Maximum aerodynamic power coefficients around 0.25 are predicted for a tip-speed ratio close to 3.0.

In addition, due to the high apparent blockage ratio of the experimental set-up, a correction has been introduced to approximate the non-dimensional performance of the turbine to real conditions (open-field). In particular, the correlations proposed in [29], have been modified to adapt some of their parameters for the studied VAWT turbine. Based on previous studies by Maskell [30], these authors presented a quadratic expression for the parameter m that it is typically used, in combination with the blockage ratio (B_R) of the wind tunnel, to "correct" the incoming flow velocity v_∞. These equations are given by:

$$\frac{v_c}{v_\infty} = \sqrt{\frac{1}{1 - mB_R}} \tag{12}$$

where.

$$m = 6.92B_R^2 - 6.76B_R + c_m \tag{13}$$

In equation (13), the independent term c_m is a function of the overall aerodynamics of the prototype, having proposed the values 3.5 for a square plate, 3.2 for a Savonius turbine and 2.8 for the straight-bladed (SB) Darrieus turbine studied in [29] (solidity $\sigma = 1.29$). Assuming an exponential-decay relationship between the parameter c_m and the

Table 3
Discrepancies in the turbine aerodynamic torque due to the overestimation of the resistant torque of the struts from uncorrected inflow velocities.

Flow deceleration (Induction factor)	0.05	0.10	0.15	0.20	0.30	0.40
Aerodynamic torque relative variation [%] (Maximum torque point-MTP)	−0.16	−1.03	−1.90	−2.78	−4.53	−6.27
Aerodynamic torque relative variation [%] (Maximum variation point-MVP)	−0.68	−1.82	−2.97	−4.11	−6.41	−8.70

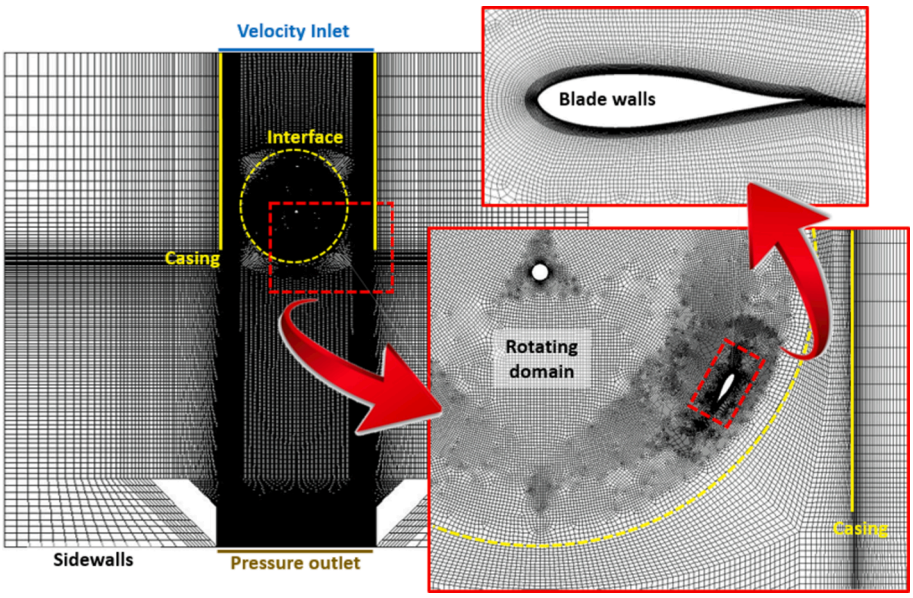

Fig. 9. Numerical 2D model of the rotating turbine: boundary conditions and mesh density.

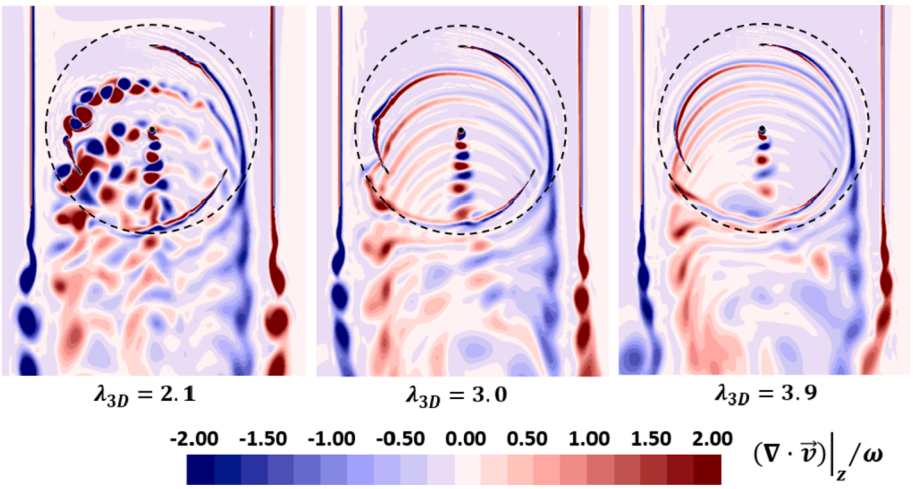

Fig. 10. Instantaneous vorticity distributions for different equivalent Tip-speed ratios.

apparent solidity of those bodies, a final value of $c_m = 1.72$ has been adopted for the VAWT of the present work (see Table 4).

Consequently, with the corrected value of the inlet velocity given by equation (12), the final performance outcome is transformed into the curve represented with the red markers in the Fig. 11. As a reference for the expected performance in open-field conditions, an analytical model of simple streamtube and actuator disc (SSTM), based on the work of Paraschivoiu [31], has been developed in MATLAB. This model has already been studied in [19] and good agreement was found with experimental data in the general trends, matching the tip-speed ratio of maximum power coefficient. The curve from this model has been included in Fig. 11, represented with a solid, doted grey line.

Note that, despite of the high blockage ratio of the experimental set-up, the correction introduced is really marginal due to the low solidity of the studied turbine with respect to the one studied in [29]. The maximum power coefficient is slightly reduced and displaced to a lower tip-speed ratio, closer to the TSR predicted by the analytical model. Although the SSTM model clearly overestimates the performance (typical of these analytical models), it is advising that the ratio v_c/v_∞ may be still higher than the optimal for the adequate blockage correction. Nevertheless, the available experimental data for the corrections used is very limited and further research is needed to evaluate the correlation between the parameter b and the turbine solidity. The methodology presented in this work can also contribute to this matter: Different turbine solidities could be achieved by modifying the airfoil chord, while only Test 2 (whole turbine with wind) would have to be performed for each new configuration.

Conclusions.

In this work, the development and application of an innovative methodology for the performance characterization of small-scale VAWT prototypes using active driving mode in wind tunnels has been presented. The proposal circumvents the typical limitations found for prototypes of reduced size when conventional passive driving mode is employed, like those related to self-starting issues, cut-in thresholds, excessive frictional losses or narrow operative ranges. Furthermore, it has been found to provide superior control of the tests with simpler and cost-effective equipment, and with a better definition of the performance curves. The ADM methodology can be easily used with complementary tests for the experimental study of the flow patterns (PIV, hot-wire, visualization techniques, etc.).

A typical experimental set-up with a DC-motor as the primary driver of a confined VAWT installed in a closed-loop wind tunnel has been

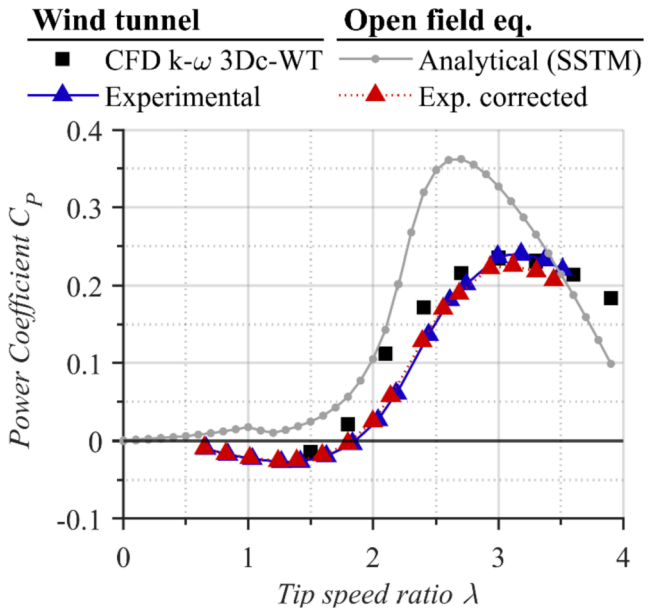

Fig. 11. Turbine performance in terms of power coefficient vs. tip-speed ratio. Comparison of 2D CFD results (open-field and confined) with respect to experimental values (original and blockage-corrected).

Table 4
Exponential fit of the parameter c_m for blockage correction.

Case	Square plate	Savonius	SB Darrieus [29]	SB Darrieus (Present work)
Solidity	∞	2	1.29	0.5
c_m	3.5	3.2	2.8	1.72

employed for the application of the methodology. Detailed uncertainty analysis has been conducted to assure the validity of the results. Four different tests were finally carried out to obtain the aerodynamic performance of the turbine from the balance of the torque outputs. According to the methodology, additional evaluation of the blades drag is required to complete the procedure.

The isolation of the blades drag from the overall mechanical losses has been identified as the most difficult challenge of the methodology. For that purpose, a 2D CFD simulation of one single rotating blade has been finally proposed as the most convenient method to estimate its contribution in terms of economy and reasonable accuracy. In addition, it has been confirmed that the influence of the strut parasitic drag must be accounted for in wind tunnel testing of small-scale prototypes for a precise determination of the aerodynamic torque. Although this parasitic drag may be affected by the flow deceleration of the turbine, it has been demonstrated that the influence of a corrected strut drag with an apparent inflow velocity is minimal. In fact, it can be neglected in the case of low-to-moderate induction factors.

To conclude, final experimental results obtained with the proposed methodology have been presented for a typical H-type VAWT turbine with three DU 06-W-200 airfoil blades. To take into account blockage effects in the wind tunnel, specific correlations for VAWT turbines have been adopted and customized for the solidity of the present design. Complementarily, a 2D URANS simulation of a similar confined layout of the turbine has been developed for validation purposes. After scaling, the numerical performance curve has been compared to the full 3D experimental results, obtaining a remarkable agreement. The final aerodynamic power coefficient of the turbine predicted by the different methodologies indicates that the experimental procedure developed for this investigation is a reliable and valuable tool for other researchers in the field.

CRediT authorship contribution statement

Luis Santamaría: Methodology, Investigation, Data curation, Writing – original draft. **Jesús Manuel Fernández Oro:** Conceptualization, Methodology, Software, Writing – review & editing, Supervision, Project administration, Writing – review & editing. **Katia María Argüelles Díaz:** Supervision, Project administration, Writing – review & editing. **Andrés Meana-Fernández:** Investigation, Software. **Bruno Pereiras:** Methodology, Resources. **Sandra Velarde-Suárez:** Supervision, Funding acquisition.

Declaration of Competing Interest

The authors declare that they have no known competing financial interests or personal relationships that could have appeared to influence the work reported in this paper.

Acknowledgements

The authors wish to thank the financial support of the Spanish Ministry of Economy, Industry and Competitiveness for the R + D Project entitled “Development and Construction of Vertical Axis Wind Turbines for Urban Environments” (DEVTURB) – Ref. ENE2017-89965-P, under the National Plan for Scientific and Technical Research and Innovation.

The grant provided by the Principality of Asturias for the support of Research Activities, funded by the Institute for Economic Development (IDEPA) under reference GRUPIN IDI/2018/000205 is also gratefully acknowledged.

Additionally, the support given by the University Institute for Industrial Technology of Asturias (IUTA) and the City Hall of Gijón, through the financed project SV-18-GIJON-1-05, is also recognized.

Finally, the authors would like to acknowledge the contributions of Prof. José González and As. Prof. Mónica Galdo for their advice and support during the measurement campaign.

References

[1] IEA. World Energy Outlook 2021 - revised version October 2021 2021.
[2] Menéndez J, Loredo J, Galdo M, Fernández-Oro JM. Energy storage in underground coal mines in NW Spain: Assessment of an underground lower water reservoir and preliminary energy balance. Renewable Energy 2019;134:1381–91. https://doi.org/10.1016/j.renene.2018.09.042.
[3] de Prado LÁ, Menéndez J, Bernardo-Sánchez A, Galdo M, Loredo J, Fernández-Oro JM. Thermodynamic analysis of compressed air energy storage (Caes) reservoirs in abandoned mines using different sealing layers. Appl Sci (Switzerland) 2021;11. https://doi.org/10.3390/app11062573.
[4] Pinto ES, Serra LM, Lázaro A. Optimization of the design of polygeneration systems for the residential sector under different self-consumption regulations. Internat J Energy Res 2020;44:11248–73. https://doi.org/10.1002/er.5738.
[5] Balduzzi F, Bianchini A, Carnevale EA, Ferrari L, Magnani S. Feasibility analysis of a Darrieus vertical-axis wind turbine installation in the rooftop of a building. Appl Energy 2012;97:921–9. https://doi.org/10.1016/j.apenergy.2011.12.008.
[6] Borg M, Collu M. A comparison between the dynamics of horizontal and vertical axis offshore floating wind turbines. Phil Trans R Soc A 2015;373(2035): 20140076.
[7] Zhao Z, Wang D, Wang T, Shen W, Liu H, Chen M. A review: Approaches for aerodynamic performance improvement of lift-type vertical axis wind turbine. Sustainable Energy Technol Assess 2022;49:101789. https://doi.org/10.1016/j.seta.2021.101789.
[8] Du L, Ingram G, Dominy RG. A review of H-Darrieus wind turbine aerodynamic research. Proc Instit Mech Eng, Part C: J Mechan Eng Sci 2019;233(23-24): 7590–616.
[9] Castelli MR, Ardizzon G, Battisti L, Benini E, Pavesi G. Modeling strategy and numerical validation for a Darrieus vertical axis micro-wind turbine. ASME International mechanical engineering congress and exposition, Proceedings (IMECE) 2010;7:409–18. https://doi.org/10.1115/IMECE2010-39548.
[10] Mertens S, Van Kuik G, Van Bussel G. Performance of an H-Darrieus in the skewed flow on a roof. J Solar Energy Eng Trans ASME 2003;125:433–40. https://doi.org/10.1115/1.1629309.
[11] Du L, Ingram G, Dominy RG. Experimental study of the effects of turbine solidity, blade profile, pitch angle, surface roughness, and aspect ratio on the H-Darrieus wind turbine self-starting and overall performance. Energy Sci Eng 2019;7: 2421–36. https://doi.org/10.1002/ese3.430.

[12] Edwards JM, Angelo Danao L, Howell RJ. Novel experimental power curve determination and computational methods for the performance analysis of vertical axis wind turbines. J Solar Energy Eng Trans ASME 2012;134:1–11. https://doi.org/10.1115/1.4006196.
[13] Araya DB, Dabiri JO. A comparison of wake measurements in motor-driven and flow-driven turbine experiments. Exp Fluids 2015;56:1–15. https://doi.org/10.1007/s00348-015-2022-7.
[14] Dou B, Yang Z, Guala M, Qu T, Lei L, Zeng P. Comparison of Different Driving Modes for the Wind Turbine Wake in Wind Tunnels n.d. https://doi.org/10.3390/en13081915.
[15] Fujisawa N, Shibuya S. Observations of dynamic stall on turbine blades. J Wind Eng Ind Aerodyn 2001;89:201–14. https://doi.org/10.1016/S0167-6105(00)00062-3.
[16] Simão Ferreira C, Van Kuik G, Van Bussel G, Scarano F. Visualization by PIV of dynamic stall on a vertical axis wind turbine. Exp Fluids 2009;46:97–108. https://doi.org/10.1007/s00348-008-0543-z.
[17] Edwards JM, Angelo Danao L, Howell RJ. Novel experimental power curve determination and computational methods for the performance analysis of vertical axis wind turbines. J Sol Energy Eng 2012;134:031008. https://doi.org/10.1115/1.4006196.
[18] Bachant P, Wosnik M. Reynolds number dependence of cross-flow turbine performance and near-wake characteristics. In: Proc of the 2nd marine energy technology symposium; 2014. p. 1–9.
[19] Meana-Fernández A, Solís-Gallego I, Fernández Oro JM, Argüelles Díaz KM, Velarde-Suárez S. Parametrical evaluation of the aerodynamic performance of vertical axis wind turbines for the proposal of optimized designs. Energy 2018;147:504–17. https://doi.org/10.1016/j.energy.2018.01.062.
[20] Santamaría L, Vega MG. Training Program for Researchers in Design and Manufacturing of Experimental Prototypes for Fluids Engineering using Additive Technologies 2021:1–8. https://doi.org/10.1088/1757-899X/1193/1/012096.
[21] Santamaría L, María K, Díaz A, Pereiras B, Vega MG, Pérez JG, et al. Preliminary flow measurements of a small-scale , vertical axis wind turbine for the analysis of blockage influence in wind tunnels. vol. AICFM16. 2022.
[22] Battisti L, Persico G, Dossena V, Paradiso B, Raciti Castelli M, Brighenti A, et al. Experimental benchmark data for H-shaped and troposkien VAWT architectures. Renewable Energy 2018;125:425–44.
[23] Rodríguez Lastra M, Fernández Oro JM, Galdo Vega M, Blanco Marigorta E, Santolaria MC. Novel design and experimental validation of a contraction nozzle for aerodynamic measurements in a subsonic wind tunnel. J Wind Eng Ind Aerodyn 2013;118:35–43. https://doi.org/10.1016/j.jweia.2013.04.008.
[24] Bianchini A, Balduzzi F, Bachant P, Ferrara G, Ferrari L. Effectiveness of two-dimensional CFD simulations for Darrieus VAWTs: a combined numerical and experimental assessment. Energy Convers Manage 2017;136:318–28. https://doi.org/10.1016/j.enconman.2017.01.026.
[25] Kline SJ. The purposes of uncertainty analysis. J Fluids Eng Trans ASME 1985;107:153–60. https://doi.org/10.1115/1.3242449.
[26] Rezaeiha A, Montazeri H, Blocken B. Towards accurate CFD simulations of vertical axis wind turbines at different tip speed ratios and solidities: Guidelines for azimuthal increment, domain size and convergence. Energy Convers Manage 2018;156:301–16. https://doi.org/10.1016/j.enconman.2017.11.026.
[27] Castelli MR, Masi M, Battisti L, Benini E, Brighenti A, Dossena V, et al. Reliability of numerical wind tunnels for VAWT simulation. J Phys Conf Ser 2016;753:082025.
[28] Claessens MC. The design and testing of airfoils for application in small vertical axis wind turbines. Masters Thesis 2006:1–137.
[29] Jeong H, Lee S, Kwon SD. Blockage corrections for wind tunnel tests conducted on a Darrieus wind turbine. J Wind Eng Ind Aerodyn 2018;179:229–39. https://doi.org/10.1016/j.jweia.2018.06.002.
[30] Maskell EC. A theory of blockage effects on bulff bodies and stalled wings in a closed wind tunnel. Her Majesty's Stat Off 1965:1–27.
[31] Paraschivoiu I. Wind Turbine Design: With Emphasis on Darrieus Concept. 2002.